Cell Cycle 9:23, 4656-4665; December 1, 2010; © 2010 Landes Bioscience

Rb-dependent cellular senescence, multinucleation and susceptibility to oncogenic transformation through PKC scaffolding by SSeCKS/AKAP12

Shin Akakura, Peter Nochajski, Lingqiu Gao, Paula Sotomayor, Sei-ichi Matsui and Irwin H. Gelman*

Department of Cancer Genetics; Roswell Park Cancer Institute; Buffalo, NY USA

Key words: SSeCKS/Akap12, PKC, senescence, MEF, Rb, *Lats1/Warts*, p16^{Ink4a}, Id1, polyploidy, binucleation

A subset of AKAPs (A Kinase Anchoring Proteins) regulate signaling and cytoskeletal pathways through the spaciotemporal scaffolding of multiple protein kinases (PK), such as PKC and PKA, and associations with the plasma membrane and the actin-based cytoskeleton. SSeCKS/Gravin/Akap12 expression is severely downregulated in many advanced cancers and exhibits tumor- and metastasis-suppressing activity. *akap12*-null (KO) mice develop prostatic hyperplasia with focal dysplasia, but the precise mechanism how Akap12 prevents oncogenic progression remains unclear. Here, we show that KO mouse embryonic fibroblasts (MEF) exhibit premature senescence marked by polyploidy and multinucleation, and by increased susceptibility to oncogenic transformation. Although p53 and Rb pathways are activated in the absence of Akap12, senescence is dependent on Rb. Senescence is driven by the activation of PKCα, which induces p16^{Ink4a}/Rb through a MEK-dependent downregulation of Id1, and PKCδ, which downregulates *Lats1/Warts*, a mitotic exit network kinase required for cytokinesis. Our data strongly suggest that Akap12 controls Rb-mediated cell aging and oncogenic progression by directly scaffolding and attenuating PKCα/δ.

Introduction

Cell senescence is controlled by p53 or pRb proteins under conditions of cell aging that include telomere shortening and increased production of reactive oxygen species (ROS), the latter triggerable by damage to proteins, nucleic acids and lipids. Sustained expression of p16^{Ink4a} and p21$^{WAF1/Cip1}$ under these stress conditions suppresses the activity of cyclin/cyclin-dependent kinase complexes, preventing hyperphosphorylation of pRb. This, in turn, facilitates growth arrest by allowing pRb to continue to suppress the E2F-mediated transcription of cell cycle progression genes. In addition, genotoxic or osmotic stress conditions can increase the stability of p53 protein through the action of the *ARF* gene product, leading to the induction of p53-regulated genes such as p21$^{WAF1/Cip1}$.[1,2] Although there is a considerable literature elucidating the downstream effectors of p53 in cell senescence,[3] the mechanism by which pRb functions in this regard is less clear.

Src-Suppressed-C Kinase Substrate (SSeCKS), encoded by the rodent orthologue of human Gravin/AKAP12, originally identified as a suppressor of v-Src oncogenic signaling,[4-6] is a major substrate of protein kinase (PK) C[6-8] and a scaffold protein for PKC and PKA.[9] Akap12 is severely downregulated by oncogenic forms of Src, Ras, Myc and Jun,[4] but not by oncogenic forms of Raf, Mos or Neu, indicating that its downregulation is not a generic effect of cell transformation. Moreover, milder downregulation of Akap12 is already manifest in clones of spontaneously-arising immortalized cells that gain permissiveness for H-Ras-induced transformation compared to primary REF52 diploid fibroblasts.[10]

There is mounting data indicating that Akap12 functions as a tumor- and/or metastasis-suppressor, including its mapping to human chromosome 6q24-5.2, a deletion hotspot in prostate, breast and ovarian cancers.[4] The tumor- and metastasis-suppressor functions of Akap12 likely involve its ability to modulate specific oncogenic signaling pathways through the scaffolding of key mitogenic regulators such as PKC, PKA, cyclins and calmodulin.[4,11-14]

We showed recently that Akap12-null (KO) mice exhibit prostatic hyperplasia along with focal dysplasia marked by the loss of inter-epithelial E-cadherin staining in the luminal layer and by the loss of HMW-cytokeratin-staining basal epithelial cells.[15] Notably, all four prostatic lobes displayed increased apoptotic indices although hypercellularity due to net cell proliferation increases was detected in the anterior and ventral lobes only. These lesions also showed significantly higher relative phospho-Akt levels, suggesting that Akap12 normally antagonizes PI3K activation pathways. Although these effects, reminiscent of

*Correspondence to: Irwin H. Gelman; Email; Irwin.Gelman@roswellpark.org
Submitted: 10/15/10; Accepted: 10/18/10
Previously published online: www.landesbioscience.com/journals/cc/article/13974
DOI: 10.4161/cc.9.23.13974

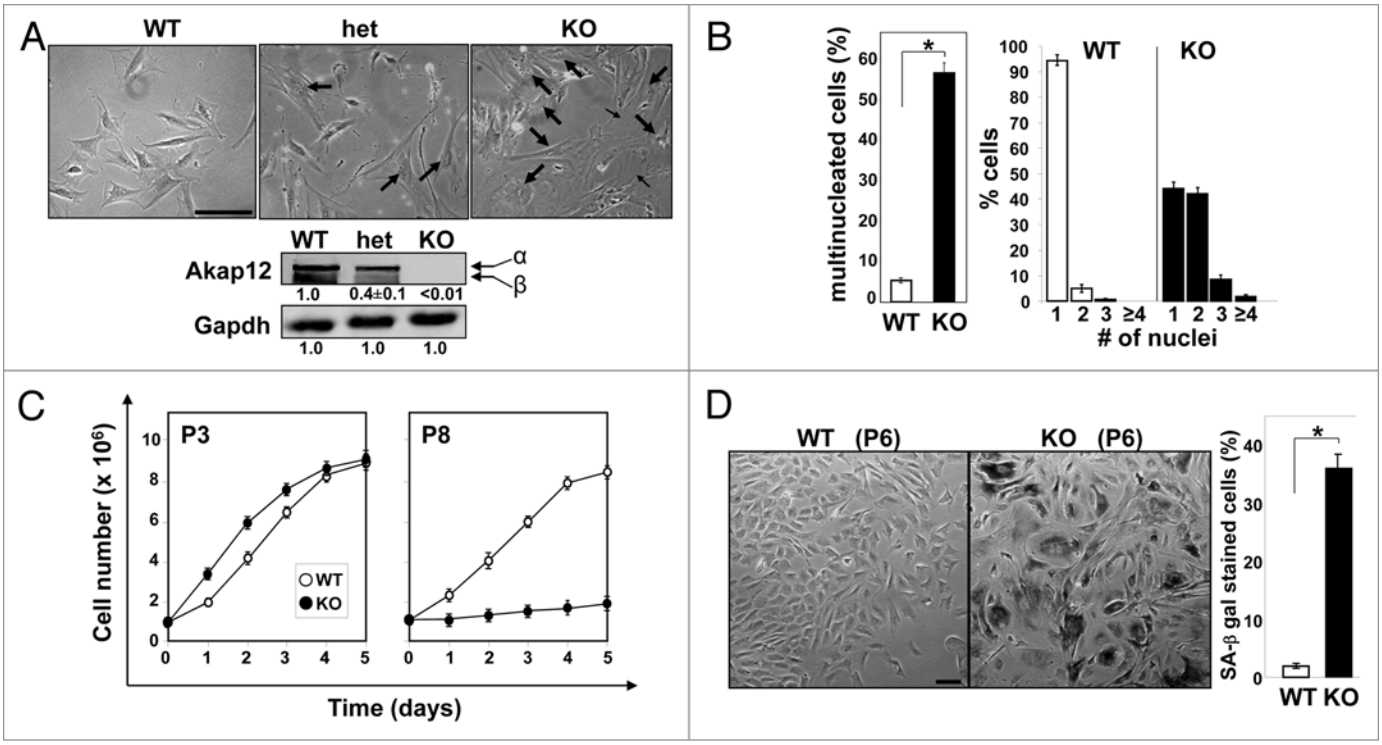

Figure 1. Loss of Akap12 leads to multinucleation, polyploidy and premature senescence. (A) Phase contrast images of Akap12$^{+/+}$, $^{+/-}$ and $^{-/-}$ (WT, het and KO) MEF (upper). Scale bar, 30 μm. Thick arrows, binucleated cells; thin arrows, stress fiber bundles. Lower: Immunoblotting of WT, het and KO MEF lysates probed for Akap12 (showing α and β isoforms) or Gapdh. (B) Percentage of multinucleated cells in WT- vs. KO-MEF (left) versus the number of the nuclei/cell (right). *p < 0.001. (C) Cell proliferation rates in P3 vs. P8 WT- and KO-MEF. (D) Left: P6 KO-MEF display premature senescence based on SAβgal staining and enlarged cell morphologies. Scale bar, 30 μm. Right: percentage of SAβgal-stained cells from P6. *p < 0.001.

a senescent state in vivo, are predicted by the loss of a tumor suppressor that regulates cell cycle progression, the precise mechanism by which Akap12 controls cell cycle or oncogenic progression remains unclear.

Here, we show that mouse embryonic fibroblasts from *akap12*-null mice (KO-MEF) exhibit polyploidy/multinucleation, increased DNA damage marker levels, increased susceptibility to oncogenic transformation and premature senescence, correlating with the activation of Rb, increases in the expression of p16^{Ink4a}, p19^{Arf}, p21$^{Waf1/Cip1}$ and p53, and decreases in the expression of CDK4 and the mitotic exit network kinase, *Lats1/Warts*. Many of these senescence markers are manifest in hyperplastic prostatic lesions in KO mice. The premature senescence in the absence of Akap12 was Rb-dependent, requiring PKCα and δ, and is likely regulated by the ability of Akap12 to control PKC activity through a direct scaffolding function. Our evidence suggests that Akap12 prevents Rb-mediated cell senescence and oncogenic progression by attenuating RB activation through a PKCα/MEK/Id1/p16^{Ink4a} pathway and by preventing downregulation of *Lats1/Warts* by PKCδ.

Results

Loss of Akap12 results in polyploidy/binucleation and premature-senescence. Akap12 negatively regulates growth factor-induced cell cycle progression,[4,16] and its loss causes hyperplastic lesions in the prostate paradoxically marked by increased levels of Akt^{poSer473} and apoptosis.[15] Given that these combined conditions are often harbingers of premature cell aging following the loss of a tumor suppressor function,[17] hyperplastic lesions from *akap12*-null (KO) mice were surveyed for markers of cell senescence. Compared to age-matched WT mice, prostates from *akap12*-null mice displayed increased senescence-associated β-galactosidase (SAβgal)[18] (**Sup. Fig. 1a**), p16^{Ink4a} (**Sup. Fig. 1b**) and a marker of DNA damage, γH2AX (**Sup. Fig. 1c**), consistent with the notion that the loss of a tumor suppressor function such as Akap12 results in both increased cell aging and proliferation.

MEF culture models have been used to dissect the senescence pathways induced by the loss of tumor suppressors,[19] and thus, we isolated MEF from WT, KO and *akap12*$^{+/-}$ ("het") mice. KO-MEF were severely flattened (**Fig. 1A**) and displayed increased production of thick, longitudinal stress fibers, non-peripheral, dorsal focal adhesion plaques (**Sup. Fig. 2**), and long cell projections (**Fig. 1A**). Het-MEF, which express roughly half the Akap12 protein level of WT-MEF (**Fig. 1A**), also exhibited increased levels of binucleation suggesting that the appropriate completion of cytokinesis and/or cell septation could be influenced by *akap12* haploinsufficiency. These structural changes parallel those produced by knocking down Akap12 in mesangial cells.[20]

The loss of Akap12 resulted in cytokinesis defects and premature senescence. Specifically, compared to WT-MEF at similar

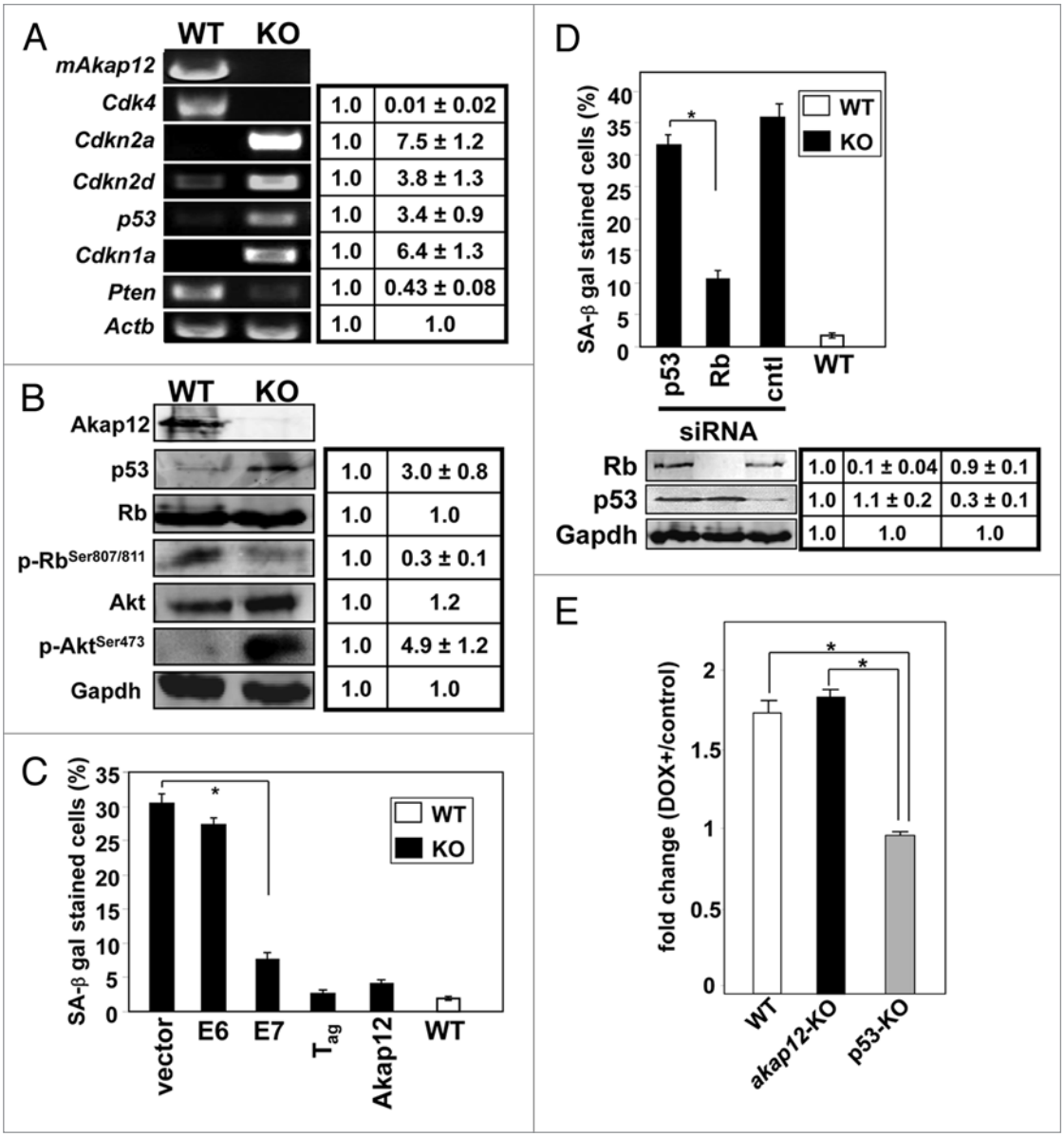

Figure 2. Loss of Akap12 activates both p53 and Rb pathways, but premature senescence in KO-MEF is Rb-dependent. (A) Left: Semi-Q RT-PCR performed on total RNA from P5 WT- or KO-MEF using gene primers described in Table 1. Right: densitometric scans of triplicate independent experiments; SE, $p < 0.01$. (B) Left: IB of P5 cell lysates probed for Akap12, p53, total Rb, $Rb^{poSer807/811}$, $Akt^{poSer473}$, total Akt or Gapdh. Right: densitometric scans of triplicate independent experiments; SE, $p < 0.01$. (C) Percentage of SAβgal staining in P4 KO-MEF (black columns) after infection with high-titer pBABE retroviruses containing empty vector, HPV16-E6, HPV16-E7, SV40-$T_{antigen}$ (SV-Tag) or Akap12, compared to the SAβgal staining of P4 WT-MEF (white column). *$p < 0.001$. (D) Upper: Percentage of SAβgal staining in P4 KO-MEF (black columns) 4 d after transfection with p53- or Rb-specific siRNA or control (scrambled) siRNA, compared to the SAβgal staining of WT-MEF (white column). *$p < 0.005$. Lower: IB of cell lysates from the upper part, probed for Rb, p53 or Gapdh. (E) p53 is active in KO-MEF. WT-, akap12 KO- or $p53^{-/-}$ MEF were transfected transiently with a p53-inducible p21-Luciferase construct and lysates were subjected to luciferase assays after treatment for 16 h with doxorubicin or vehicle. Error bars, SE; *$p < 0.005$.

early passages, KO-MEF exhibited severe multinucleation and polyploidy. Multinucleation in KO-MEF was 10.2-fold higher than in WT-MEF (57.1% ± 3.0 versus 5.6% ± 0.8; **Fig. 1B**, left part), with roughly 90% of the multinucleation representing binucleated cells (**Fig. 1B** and right part). Flow cytometric analysis of propidium iodide-labeled cells indicated that KO-MEF had relative increases in their tetraploid and octaploid populations, with a concomitant decrease in the 2N population, yet a slight increase in sub-2N-containing cells typically thought to be apoptotic (**Sup. Fig. 3a**). These findings were also confirmed by chromosome counting of fixed metaphase spreads: by passage (P)2, roughly 50–60% of KO-MEF were tetraploid whereas 4–5% were octaploid (**Sup. Fig. 3b**). Little aneuploidy was found, strengthening the notion that the loss of Akap12 caused cytokinesis defects rather than specific mistakes in chromosomal segregation.

Because *akap12*-null mice have higher relative proliferation in luminal prostate cells compared to WT mice,[15] and because of

the known role of Akap12 in regulating cell cycle progression,[16] we compared the proliferation rates of WT- vs. KO-MEF. Early-passage (P3) KO-MEF proliferated at faster rates than WT-MEF, whereas by P8, the KO-MEF had lost all proliferative capacity (**Fig. 1C**). Indeed, P6 KO-MEF showed significantly increased SAβgal levels (36.3% ± 3.6 in KO-MEF vs. 3.4% ± 0.5 in WT-MEF), a well-established marker of senescence,[18] as well as increased cell flattening (**Fig. 1D**). Taken with the finding that KO-MEF exhibited increased levels of intranuclear focal staining for γH2AX (**Fig. S4**), a senescence-associated DNA damage marker,[2] these data strongly suggest that the growth arrest of the KO-MEF reflects premature senescence.

In order to confirm that the premature senescence in KO-MEF is due to Akap12 deficiency, WT-MEF were treated with murine-specific *akap12* siRNA ("si-mAKAP12") followed by SAβgal staining. Akap12 knockdown, confirmed by immunoblotting (**Sup. Fig. 5a** and lower part), resulted in a 5-fold increase in SAβgal staining (2.4% ± 0.9 with vs. 12.1% ± 2.3 with si-mAKAP12; **Sup. Fig. 5a**, upper part). Similarly, the siRNA-mediated knockdown of human *AKAP12* ("si-hAKAP12") in human diploid fibroblasts (IMR90) resulted in a 4.4-fold increase in SAβgal staining (**Sup. Fig. 5b**). Thus, AKAP12 deficiency in primary diploid fibroblasts is sufficient to induce senescence.

Premature senescence in *akap12*-null-MEF is Rb-dependent. p53 and Rb are major mediators of cellular senescence along with CKIs such as $p16^{Ink4a}$, $p19^{Arf}$ and $p21^{Waf1/Cip1}$.[21] We examined a select panel of senescence-regulating genes by semi-Q RT-PCR for differential expression in passage-matched pre-senescent KO- vs. WT-MEF. RNA accumulation levels for *Cdk4* were severely decreased, and *Cdkn2a* ($p16^{Ink4a}$), *Cdkn2d* ($p19^{Arf}$), *p53* and *Cdkn1a* ($p21^{Waf1/Cip1}$) RNA levels were increased in the absence of Akap12 (**Fig. 2A**). A relative increase in p53 protein levels in KO-MEF was confirmed by IB (**Fig. 2B**). Although the total Rb protein levels did not change, RB was relatively underphosphorylated in KO-MEF, suggesting higher E2F-suppressing activity.[22]

The increased relative levels of Akt phosphorylation in KO-MEF (**Fig. 2B**) parallel those found in the hyperplastic prostates of KO mice[15] and correlate with the decreased levels of *Pten* RNA (**Fig. 2A**). Previous reports have linked AKT with p53-mediated senescence,[23] but there is scant literature addressing the role of AKT in Rb-mediated senescence. Moreover, the increased levels of *Cdkn2a* RNA, encoding $p16^{Ink4a}$, and decreased levels of *Cdk4* (**Fig. 2A**), correlate with the increased Rb activation levels in the KO-MEF, and are consistent with the increased levels of $p16^{Ink4a}$ in the KO prostate lesions (**Sup. Fig. 1b**). Taken together, these data demonstrate that the loss of Akap12 leads to the activation of both p53 and Rb pathways.

To examine whether the senescence caused by loss of Akap12 is p53 or Rb-dependent, p53 or Rb function was inhibited in KO-MEF using viral antagonist proteins, or p53/Rb expression was knocked down using specific siRNAs. As a control, the re-expression of Akap12 could decrease senescence to the levels found in passage-matched WT-MEF (2.5% ± 0.6 vs. 1.8% ± 0.3, respectively) (**Fig. 2C**). Transduction of KO-MEF with HPV16-E7, which inhibits Rb function, or SV40-$T_{antigen}$, which inhibits both p53 and Rb, suppressed senescence levels. In contrast, cells infected with pBABE or virus encoding HPV16-E6, which inhibits p53, remained highly senescent (**Fig. 2C**). Similarly, the knockdown of Rb, but not p53, suppressed senescence in the KO-MEF (**Fig. 2D**). The failure of the p53-siRNA to suppress senescence was an important control because HPV16-E7 partially suppresses p53-mediated senescence through a direct binding to p21.[24] Interestingly, our data suggest that p53 remains active in the KO-MEF because of the upregulation of *Cdkn1a* (**Fig. 2A**) and the p53-dependent, stress-induced induction of a luciferase reporter driven by the $p21^{Waf/Cip1}$ promoter (**Fig. 2E**). These data are consistent with an Rb-dependent, p53-independent senescence in KO-MEF.

Akap12 scaffolding of PKC isozymes controls senescence. Akap12 directly scaffolds PKC isozymes[6-9,13,25] such that saturated binding inhibits PKC kinase activity.[6,8,9] Moreover, activated PKCα, δ and ε isozymes play direct roles in inducing cell senescence and cytokinesis defects.[2] Thus, we examined whether Rb-dependent senescence in the KO-MEF is driven by hyperactive PKC resulting from the loss of Akap12 scaffolding activity. Akap12 can be co-immunoprecipitated with HA-tagged PKCα, δ and ε isozymes in HEK293T transient overexpression assays (**Fig. 3A**). Total PKC kinase activity was increased in KO vs. WT-MEF 2.2-fold (**Sup. Fig. 6a**), and inhibition of PKC kinase activity with the pan-PKC inhibitor, *bis*-indolylmaleimide (BIM), reduced senescence in a dose-dependent manner (**Sup. Fig. 7**), demonstrating that the senescence in KO-MEF is regulated by PKC. Interestingly, isozyme-specific in vitro kinase assays of immunoprecipitated PKC identified increased relative kinase activities for PKCα and δ only (3.3- and 1.8-fold increases, respectively) in KO- vs. WT-MEF (**Fig. 3B**). We used several other assays to confirm the higher PKCα and δ activation in KO-MEF. Specifically, PKCα could spontaneously localize to plasma membrane sites in KO-, but not in WT-MEF, in a kinase-dependent manner (**Sup. Fig. 6b**) and KO-MEF displayed significantly higher levels of the so-called PKCδ-CF ("cleaved fragment"), reflecting cleavage by caspase-3 of only kinase-active forms (**Sup. Fig. 6c**). Importantly, senescence in KO-MEF could not be suppressed by Akap[Δ553-900], a mutant deleted of its PKC binding domain (**Fig. 3C**) (Li-wu Guo, Bing Su, Lingqiu Gao and Irwin H. Gelman, "SSeCKS/AKAP12 transduces phorbol ester-induced cytoskeletal remodeling and cell survival signals by scaffolding PKC," submitted for publication). Moreover, the RNAi-mediated knockdown of PKCα and δ, but not PKCε, decreased premature senescence in KO-MEF (**Fig. 3D**). These data strongly suggest that SSeCKS prevents premature senescence by attenuating PKCα and δ activity through direct scaffolding.

The upregulation of $p16^{Ink4a}$ is sufficient to induce senescence and multinucleation.[26] Expression of p16 is regulated positively or negatively, respectively, by Ets2 or Id1.[27] Compared to transcript levels in WT-MEF, *Id1* transcript levels were severely downregulated in KO-MEF, whereas *Ets2* transcript level were unaffected by Akap12 loss (**Fig. 4A**). This agrees with data from our Affymetrix microarray analysis comparing differential gene expression in P4 KO- vs. WT-MEF, namely 14.63-fold lower *Id1* in KO-MEF ($p = 1.48 \times 10^{-20}$) and no significant change in *Ets2* ($p = 0.0216$). Activated MEK-ERK signaling has been shown to suppress *Id1*

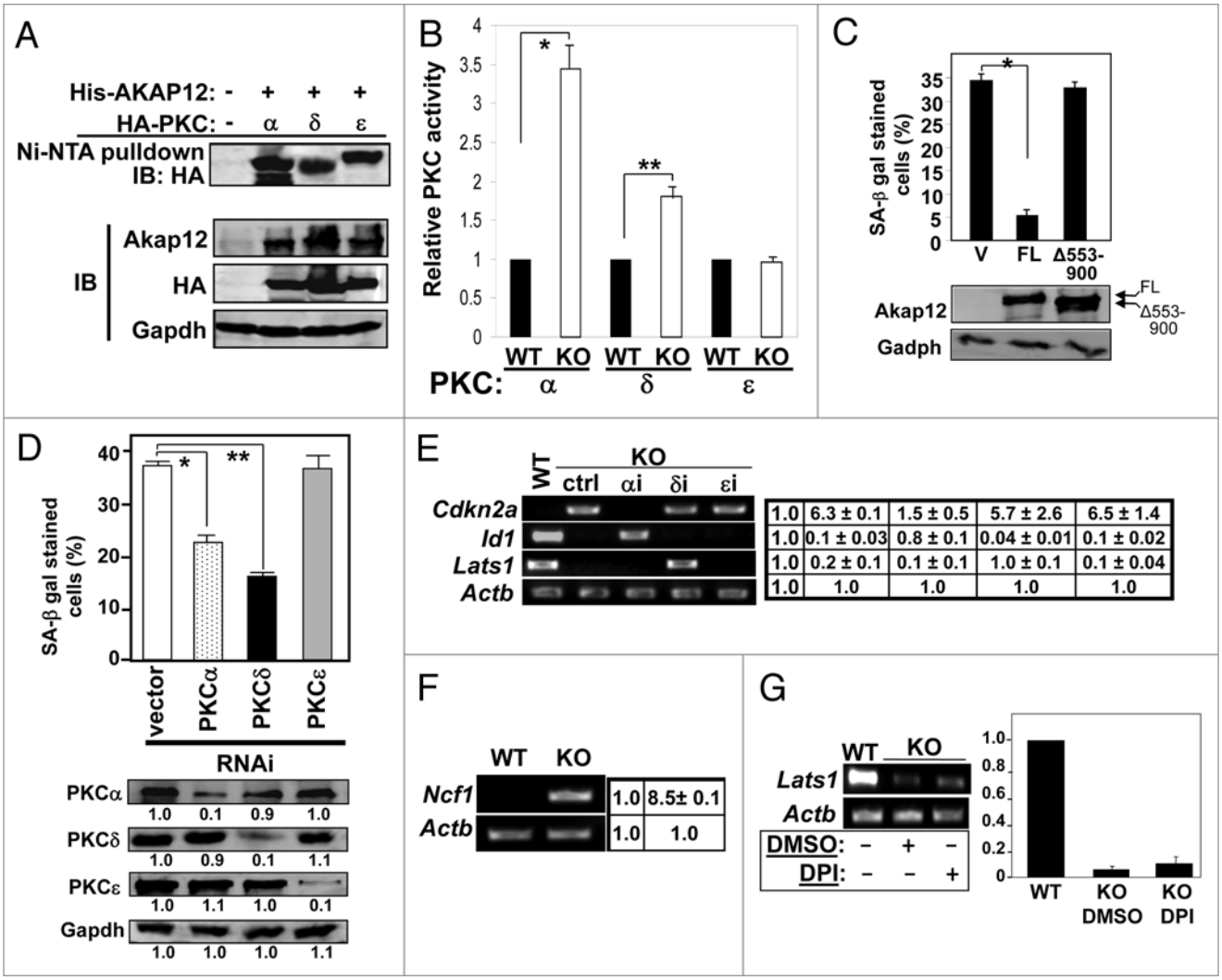

Figure 3. Akap12 binds to PKC and regulates its activity. (A) Lysates from 293T cells transfected with His-Akap12 and HA-PKCα, δ or ε were incubated with Ni^{2+}-NTA resin and subjected to immunoblotting for the HA-tag (upper) or to direct immunoblotting for Akap12, HA and Gapdh (lower). (B) Relative activities of PKCα, δ or ε in WT- vs. KO-MEF. Relative kinase activity was defined as the amount of labeled substrate normalized to the amount of PKC isozyme in immunoprecipitates (Fig. S11). *p < 0.005; **p < 0.01. (C) Upper: Percentage of SAβgal-stained P4 KO-MEF infected with pBABE vector (V), pBABE-Akap12 full length (FL) or pBABE-Akap12(Δa.a.553–900). Lower: IB of FL and Δ553–900 expression in the transfected KO-MEF probed for Akap12 or Gapdh. (D) Upper: Percentage of SAβgal-stained cells 5 d after transfection with PKCα-specific siRNA or infection with high-titer virus encoding PKCδ- or ε -specific shRNA. *p < 0.01; **p < 0.005. Lower: IB of KO-MEF lysates from the upper part, probed for PKCα, δ or ε or Gapdh. (E) The effect of PKC isozyme knockdown in P4 KO-MEF on $p16^{Ink4a}$ (Cdkn2a), Id1 or Lats1 transcript levels (vs. Actb controls). ctrl, scrambled siRNA; αi, siRNA-PKCα; δi, shRNA-PKCd; εi, shRNA-PKCε. These results are typical of three independent experiments. (F) Increased Ncf1 transcript levels, encoding $p47^{Phox}$, in KO- vs. WT-MEF. (G) The NADPH oxidase inhibitor, DPI (10 μM for 3 h), fails to increase Lats1 transcript levels in KO-MEF. Left part- Semi-quantitative RT-PCR of total RNA from P4 WT- or KO-MEF treated with DMSO or DPI, using Lats1 or Actb primer set. Right part-average of three independent experiments; error bars, SE; *p < 0.01.

expression.[28] Given that Akap12 inhibits serum-induced activation of MEK-ERK signaling,[12] we assessed relative phospho-MEK1/2 levels in serum-starved WT- and KO-MEF treated short term with 10% FBS. Consistent with our previous findings, both the basal and serum-induced levels of activated MEK were higher in KO- vs. WT-MEF (**Fig. 4B**). As a control, Akap12 did not alter total MEK protein levels in the absence or presence of serum (**Fig. 4B**). Treatment of KO-MEF with the MEK inhibitor, U0126, induced *Id1* expression and suppressed *Cdkn2a* levels (**Fig. 4C**), consistent with the notion that *Id1* downregulation in KO-MEF is caused by hyperactive MEK and that Id1 suppresses *Cdkn2a* transcription. Moreover, inhibition of MEK decreased senescence in KO-MEF (**Fig. 4D**), underlining the importance of the p16/Rb axis in inducing senescence in this context. Lastly, whereas the knockdown of PKCα by siRNA had the same effect as MEK inhibition, namely increased *Id1* and decreased *Cdkn2a* levels, knockdown of PKCδ or ε had no effect on these RNA levels (**Fig. 3E**). In contrast, the knockdown of PKCδ, but not PKCα or ε, resulted in the re-expression of *Lats1/Warts*, encoding a kinase required for completion of mitosis[29] (**Fig. 3E**). Loss of this kinase is known to lead to cytokinesis defects that result in binucleation and polyploidy,[29,30] and thus, it is possible that its

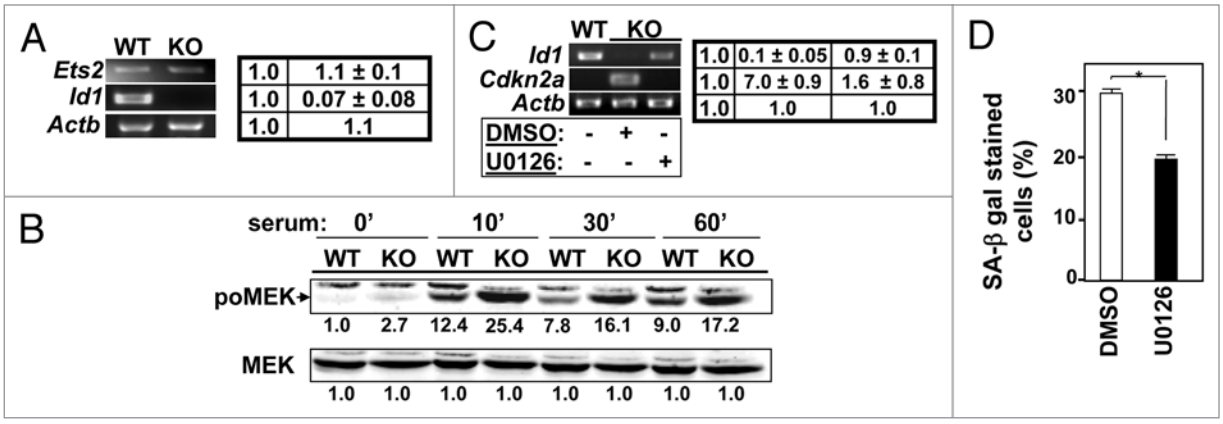

Figure 4. Premature senescence in KO-MEF is driven by hyperactivated MEK. (A) Semi-Q RT-PCR of total RNA from (P4) WT- or KO-MEF assessed for Ets2 and Id1, with β-actin RNA as a control. Right-densitometric scans of triplicate independent experiments; SE, $p < 0.01$. (B) Lysates of serum-starved MEFs treated with 10% FBS for various time intervals were probed by IB for total MEK1/2 and MEK$^{poSer218/222}$. (C) Semi-Q RT-PCR analysis of Ets2, Id1 and Actb RNA levels in P4 WT-MEF compared to KO-MEF treated with U0126 or DMSO vehicle. Right-densitometric scans of triplicate independent experiments; SE, $p < 0.01$. (D) Percentage of SAβgal-stained KO-MEF treated overnight with DMSO or U0126. *$p < 0.01$.

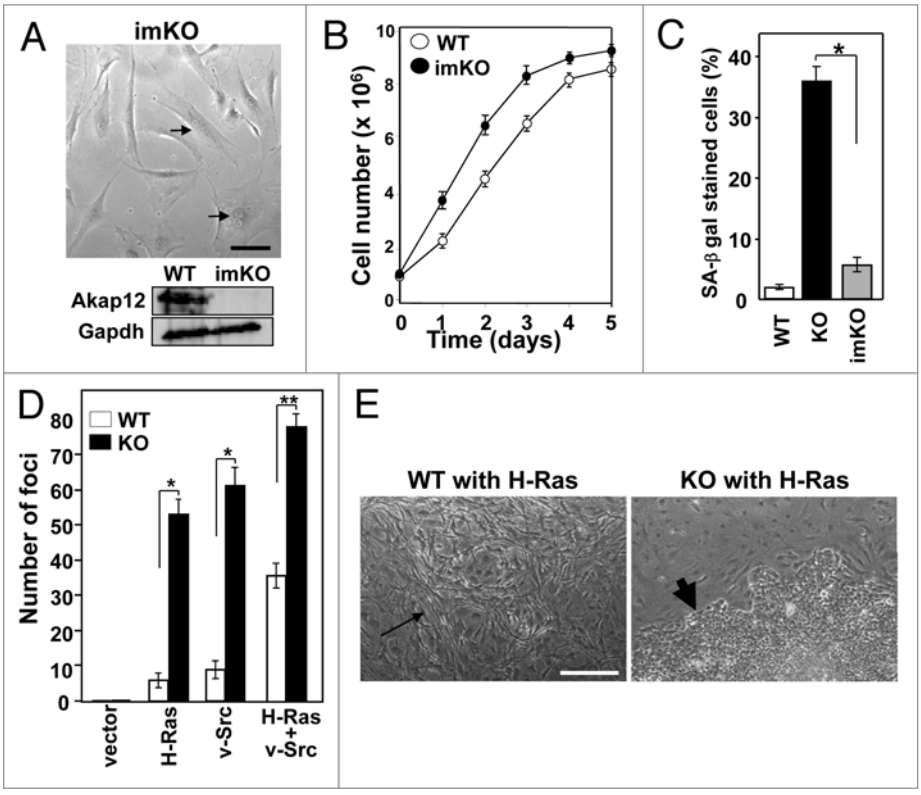

Figure 5. Loss of Akap12 causes increased susceptibility to oncogenic transformation. (A) Immortalization of KO-MEF (imKO). Upper: Representative image of imKO clone 4 (P25). Arrows, multinucleation. Size bar, 30 μm. Bottom: IB of WT-MEF (P6) and imKO (P25) probed for Akap12 or Gapdh. (B) Cell proliferation in P6 WT-MEF vs. P25 imKO. (C) Percentage of SAβgal staining in WT- (P6), KO-MEF (P6) and imKO (P25). *$p < 0.001$. (D) Comparison of the number of foci (>2 mm) from oncogene-transduced WT- or KO-MEF. *$p < 0.001$; **$p < 0.005$. (E) Phase contrast images of H-Ras(V12)-induced foci in WT- (upper; thin arrow) vs. KO-MEF (lower; thick arrow). Size bar, 50 μm.

decreased expression in KO-MEF causes the G_2/M checkpoint defects that trigger senescence. Takahashi et al.[31] showed that activated PKCδ can partially drive senescence through a positive feedback loop involving the activation of reactive oxygen species (ROS) in response to DNA damage due to the loss of *Lats1/Warts*. Analysis of differential expression between WT- and KO-MEF by Affymetrix oligonucleotide microarray indicated that p47phlox (encoded by *Ncf1*), a component of NADPH oxidase involved in ROS signaling,[1] is upregulated 8- to 13-fold in KO-MEF, a finding confirmed by semi-Q RT-PCR (**Fig. 3F**). Addition of diphenylene iodonium (DPI), an inhibitor of NADPH oxidase, partially derepressed *Lats1/Warts* expression in the KO-MEF (**Fig. 3G**), suggesting that increased ROS was responsible, in part, for *Lats1/Warts* downregulation in KO-MEF. Taken with the data above, our findings strongly suggest that the loss of Akap12-mediated scaffolding of PKC in the KO-MEF leads to hyperactivated PKC isozymes and a NADPH oxidase-associated ROS pathway that induce senescence by *Lats1/Warts* downregulation.

Loss of Akap12: cell immortalization and oncogenic predisposition. Another hallmark of cells that lose tumor suppressor functions is the propensity to gain immortalization in culture and an increased predisposition to oncogenic transformation.[32] Indeed, the ability of human prostate epithelial cells to overcome senescence and gain immortality involves the loss of p16/Rb signaling.[33] We could readily establish immortalized (im) *akap12*-null MEF, derived as proliferating colonies amongst

senescent KO-MEF, which we named imKO (**Fig. 5A**). The imKO clones grew faster than early-passage WT-MEF (**Fig. 5B**), and roughly 20% of the total cells were multinuclear (**Fig. 5A** and arrows). These cells typically had single nuclei with stable, yet slightly sub-tetraploid genomes (76 to 78 chromosomes/cell; **Sup. Fig. 8**). The imKO had severely decreased levels of senescence as gauged by SAβgal staining (**Fig. 5C**). Several imKO clones studied showed little loss of proliferative activity after 30 continual passages in culture, strongly suggesting that the imKO cells are immortalized. Moreover, whereas the enhanced p53 RNA levels found in KO-MEF were sustained in imKO, consistent with the notion that senescence in this context is p53-independent, *Cdkn2a* was downregulated and *Cdk4* was upregulated in imKO cells (**Fig. S9**). These data strengthen the notion that a p16-Rb pathway must be suppressed in order to allow for sustained proliferation after senescence. Interestingly, *Lats1/Warts* expression, downregulated in KO-MEF, is upregulated in imKO cells (**Fig. S9**).

We then examined whether KO-MEF have enhanced susceptibility toward oncogenic transformation. Thus, pre-senescent WT-MEF and KO-MEF infected with retroviruses encoding H-RasV12 and/or v-Src were subjected to focus-formation assays. Single oncogenes induced small numbers of foci in the WT-MEF whereas combining both Ras and Src oncogenes induced 5- to 7-fold higher levels of focus-formation (**Fig. 5D**). In contrast, the same single oncogenes induced 9- to 10-fold higher levels of focus-formation in the KO-MEF than in WT-MEF. Indeed, these levels in KO-MEF were close to saturation because the combination of Ras and Src only induced 30–50% more oncogenic transformation than the single oncogenes. In order to show that the transformation differences between the WT- and KO-MEF did not reflect variations in retrovirus infectivity, these cells were infected with equal titers of pBABE/GFP retrovirus (MOI = 0.5), and after two days, there were statistically equal numbers of GFP-labeled cells (WT: 55%; KO: 52%). Interestingly, the morphologies of the H-Ras-transformed WT- or KO-MEF cells differed: the *akap12*$^{+/+}$ cells were spindle-like and grew in multiple layers whereas the *akap12*-null cells were rounded and grew in compacted, non-overlapping bundles (**Fig. 5E**). In addition, KO-MEF displayed increased serum-independent growth (**Fig. S10**), possibly relating to the facile selection for populations of p16-negative immortalized KO-MEF (above), which would be expected to gain growth factor independence. These data demonstrate an enhanced susceptibility towards oncogenic transformation in the absence of Akap12.

Discussion

Although the role of Rb in mediating cell senescence is well established, with evidence that it can be mediated by hyperactivation of specific PKC isozymes and ROS,[3] little is known regarding the proteins that function upstream of these pathways during senescence. The current study strongly suggests that Akap12/Gravin/SSeCKS can normally attenuate PKC isozyme and ROS activation through direct scaffolding of PKC isozymes, such that its absence leads to senescence involving PKCα and δ.

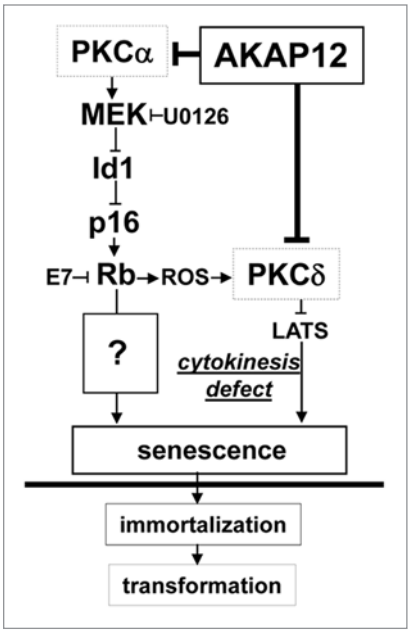

Figure 6. Model of Akap12 regulation of senescence through PKC isozyme scaffolding.

There is mounting evidence that Akap12 functions as a tumor- and metastasis-suppressor, possibly depending on tissue context. Consistent with this notion, *akap12*-null mice exhibit prostatic hyperplasia and dysplasia, marked by increased proliferation and apoptosis in the luminal epithelial cells in all four prostate lobes.[15] KO-MEF exhibit premature senescence correlating with polyploidy and multinucleation, suggesting G_2/M checkpoint defects likely involving dysfunctional cytokinesis.

Hyperactivated PKC isozymes such as α, δ or ε regulate cytokinesis completion by controlling the timing of actin-myosin ring contraction at the ingression furrow through the spatiotemporal recruitment and activation of factors such as RhoA and the Rho exchange factor Ect2 and the cofilin kinase, LIMK.[34-36] There is clear evidence that Akap12 associates with an actin-based cytoskeleton and is capable controlling cytoskeletal architecture,[16,20,37-39] and consistent with this notion, we show here that KO-MEF contain increased numbers of focal adhesion plaques and thicker, longitudinal F-actin stress fibers. A recent report identifying a pool of Akap12 staining along the actin-rich ingression furrow in anaphase[40] strengthens the notion that Akap12 normally controls parameters of cytokinesis completion. Thus, it is conceivable that a pool of Akap12 might regulate the localization and activity of PKC pools and in turn, actomyosin contraction dynamics during cytokinesis.

Although both p53- and Rb-pathways were upregulated upon loss of Akap12, our data indicate that the senescence is only Rb-dependent. This correlated with increased expression of $p16^{Ink4a}$, $p19^{Ink4d}$ and $p21^{Cip1/Waf1}$ and decreased of Cdk4. Immortalized KO-MEF clones exhibited downregulated expression of $p16^{Ink4a}$, upregulated Cdk4, but no change in p53 expression, strongly suggesting that immortalization involved suppression of Rb, but not p53. Consistent with Akap12

Table 1. Primer sequences

AKAP12 (SSeCKS)	Forward: 5'-CCC CTG AGA AAC TGG CTG AGA CCC AGG AGG TCC CCC-3' Reverse: 5'-GGG TGC TTC CGA TGG CCC CTT CTC CAG ACA CGC-3'
Cdk4	Forward: 5'-GGG CCT TCC CGT CAG CAC AGT TCG TGA GGT GGC C-3' Reverse: 5'-GCA CCA CTG ACT GCA CTG GCC GAG GCC CTC TGG G-3'
Cdkn2a (p16)	Forward: 5'-CCG CTG AGG GAG TAC AGC AGC GGG-3' Reverse: 5'-CCA TTA TTC CCT TCG CGG CCG CCT TCG C-3'
Cdkn2d (p19)	Forward: 5'-CGA TCC CGG AGA CCC AGG ACA GCG-3' Reverse: 5'-CGG TCT GGG CGA CGT TCC CAG CGG-3'
p53	Forward: 5'-GCC TCG AGC TCC CTC TGA GCC AGG-3' Reverse: 5'-GGC TCC CAG CTG GAG GTG TGG CGC-3'
Cdkn1a (p21)	Forward: 5'-CCG CAC AGG AGC AAA GTG TGC CGT-3' Reverse: 5'-CGG GGA ATC TTC AGG CCG CTC AGA-3'
Pten	Forward: 5'-GCC ACA GGC TCC CAG ACA TGA CAG CCA TCA TCA-3' Reverse: 5'-GAG GGA ACT CAA AGT ACA TGA ACT TGT CCT CCC-3'
Lats1 (WARTS)	Forward: 5'-GCC ATC CAA GGC TTC CAC CCA GGG-3' Reverse: 5'-GCC CAA CAC ATG TAA TGG GTG GGC-3'
Ncf1 ($p47^{phox}$)	Forward: 5'-CCC TGC TGG GCT TCG AGA AGC GCT TCA TCC CCA-3' Reverse: 5'-CAG CAG GTG TGG GCA GCG GGA GAT CTT CAC GGG-3'

functioning as a tumor suppressor, KO-MEF have increased susceptibility towards oncogenic transformation.

Our data suggest two roles for Akap12 in preventing senescence and oncogenic transformation through the scaffolding of specific PKC isozymes. Specifically, loss of Akap12 leads to: (i) hyperactivated PKCα, leading to MEK-mediated *Id1* downregulation, resulting in increased $p16^{Ink4a}$ expression and ultimately, Rb activation levels and (ii) hyperactivated PKCδ, which induces cytokinesis defects by downregulating *Lats1/Warts* (**Fig. 6**). The KO-MEF senescence pathways are strikingly similar to those described by Takahashi et al.[41] in regards to downregulated *Lats1/Warts* and *Cdk4* and upregulation of $p16^{Ink4a}$, Rb activity and ROS generation (through increased $p47^{phox}$ expression). Although PKCα and δ seemed to play direct roles in inducing premature senescence in our MEF system, we cannot rule out that the hyperactivation of additional PKC isozymes contribute to prostate cancer progression in the context of Akap12 downregulation. For example, current data suggest that activated PKCε drives CaP progression in vivo whereas PKCδ and possibly α, drive apoptosis.[2]

Materials and Methods

Cell culture and reagents. All chemicals were purchased from Sigma unless stated otherwise MEF were cultured in DMEM supplemented with 10% heat-inactivated bovine serum (FBS; Invitrogen), non-essential amino acids, glutamine, 2-mercaptoethanol (Invitrogen) with initial passages plated on gelatinized flask (0.2% gelatin solution, filter sterilized). Phoenix packaging cells[42] were maintained in DMEM supplemented in 10% FBS.

Plasmids and siRNA. pBABE-neo, pBABE-neo-SSeCKS(Akap12), pBABE-neo-v-Src, pBABE-neo-large T antigen and pBABE-puro-H-Ras(V12) were described previously.[43-47] pEGFP-SSeCKS (full-length and the Δ553–900 mutant) were described previously in reference 12. pET-His-Akap12/SSeCKS was generated by PCR amplification of the SSeCKS coding sequence using the following primers: forward (5'-CGG GAT CCT ACG CAC GAG CAG CAG CAC GAC AGG CCG AGC AGG CGC AGG CAG TTC CAC C-3') and reverse (5'-GGA ATT CCT TTG GTC CGT TGG TGT C-3'), and following sequence verification, the product was subcloned into BamHI/EcoRI-cut pET28a. The S*al*I/H*ind*III HPV16-E6 insert (Addgene; plasmid 8642), the E*coR*I/X*ho*I HPV16-E7 insert (Gyorgy Veress, University of Debrecen, Hungary) and the S*al*I/H*ind*III HPV16-E6 insert (Addgene; plasmid 8642) were subcloned into pBABE-neo. GFP fusions of PKCδ and ε were gifts of Jae-Won Soh (Inha University, Korea). Mouse or human AKAP12-siRNA (sc-44761 or sc-40305, respectively), Rb-siRNA (sc-29469), p53-siRNA (sc-29436) and control-siRNA (sc-37007) were obtained from Santa Cruz Biotechnology. Mouse PKCα siRNA sense and anti-sense strands according to Iwabu et al.[48] were synthesized by IDT, shRNA plasmids specific for mouse PKCδ were provided by Kaoru Hazeki (Hiroshima, Japan),[49] and pSM2 retrovirus constructs encoding mouse PKCε -specific shRNAs (Open Biosystems; clones V2MM_66391, _64658, _65184, _64091, _81431) were provided by the RPCI-UB shRNA Core Resource Lab (Irwin Gelman, Director). Transfection of siRNA samples was performed following manufacture instruction using OligofectAMINE (Invitrogen).

His-Akap12/SSeCKS purification. Protein was purified from transformed *E. coli* BL21 as described previously in reference 6.

Immunoblotting (IB). IB was performed as described previously in reference 5, using various primary antibodies (Ab) plus either anti-rabbit or -mouse IgG Alexa680 secondary Ab, and visualized using an Odyssey Infrared Imaging System (LI-COR Biosciences). Primary Ab were obtained from the following vendors; p53 (FL393; sc-6243), Rb (C-15; sc-50), p16 (sc-1661), PKCδ (sc-937), PKCε (#sc-214) and GAPDH (sc-25778) were from Santa Cruz Biotechnology; Akt (#9272), $Akt^{poSer473}$ (#9271), γH2AX (#2577), PKCα (#2056), MEK1/2 (#9122), $MEK1/2^{poSer217/221}$ (#9121) and $Rb^{poSer807/811}$ (#9308) were from Cell Signaling Technology; vinculin (#V9264) was from Sigma; paxillin (AHO0465) and GFP (A6455) were from Invitrogen; and anti-SSeCKS rabbit polyclonal Ab was described previously in reference 6.

Immunohistochemistry (IHC) and immunofluorescence analysis (IFA). Staining of formalin-fixed mouse prostate tissues was performed by the Immunohistochemistry Lab of the RPCI Pathology Resource Network (Carl Morrison, Director), using standard techniques and counterstaining with Mayer's hematoxylin. IFA was performed as described previously in reference 30.

Flow cytometry. Flow cytometry was performed using propidium iodide (PI) staining, as previously described in reference 45, at the RPCI Flow & Image Cytometry core resource (Paul

Wallace, Director) using a FACS Caliber (BD Biosciences). The data were analyzed using Cell Quest software (BD Biosciences).

Promoter luciferase assay. WT-, *akap12* KO- and p53 KO-MEF (provided by Andrei Gudkov, RPCI) were seeded onto the 10cm dish at a density of 5 x 10^5 cells per plate. Twenty-four hours after plating, 3 μg of the p53-responsive p21-Luciferase plasmid DNA (provided by Andrei Gudkov, RPCI) was transfected using Lipo293D reagent according to manufacturer's instruction (SignaGen Laboratories). 18 h after transfection, the cultures were split into 6-well plates and treated with 1 μM Doxorubicin or PBS vehicle for 16 h. Luciferase activity was determined with the Dual-Luciferase reporter assay system (Promega) according to manufacturer's instructions.

Chromosome analysis. Cells were harvested by trypsinization following colcemid-induced mitotic block, hypotonic treatment and fixation in a glacial acetic acid/methanol mixture (1:3), and were spread on glass slides either using the method which permits a preservation of cytoplasmic membranes for a validation of multi-nucleation events[51] or air-drying methods with which chromosome number can be determined.[52] Nuclei and chromosomes were stained with DAPI and their images were captured using SKYView software (v1.62) under a Nikon fluorescence microscope equipped with a triple-band filter module.

Senescence-associated β-galactosidase (SAβgal) staining. Senescence was monitored by SAβgal staining as previously described in Dimri et al.[18] For tissue SAβgal staining, prostates from were mounted in ice-cold FSC22 (Surgipath Medical Industries), and 4 μm frozen sections were cut, fixed in 1% formalin for 1 min, and incubated in SAβgal solution (pH 6.0) at 37°C for 16 h, followed by eosin counterstaining. The tissues were imaged using an Olympus BX45 microscope (Olympus) equipped with a DP25 camera (Olympus), and data were analyzed using DP2-BSW software.

Semi-quantitative (semi-Q) RT-PCR. Total RNA was prepared by standard TRIZOL-based methods (according to the manufacturer's specifications). Reverse transcription was performed according to the manufacturer's instructions (Fermentas). PCR reactions were performed using *Taq* DNA polymerase (New England Biolabs) using the following parameters: hotstart, followed by 25–30 cycles of 95°C (30 s), 55°C (30 s) and 72°C (45 s). PCR products were resolved on agarose gels followed by ethidium bromide staining. The primer sequences are described in **Table 1**.

Retrovirus infection. Phoenix packaging cells were transfected with pBABE plasmids in LipoD293 and incubated at 32°C in 5% CO_2 for 72 h. The virus-containing supernatants were added to cultures of target cells in 4 μg/ml polybrene (Sigma), and the media was replaced after 4–6 h.

Focus-formation assay. Cells infected with pBABE viruses were replated in triplicate 100 mm dishes at 5 x 10^5 cells/dish, incubated for 2 weeks (with frequent replenishment of media), fixed with 100% methanol and stained with crystal violet. Transfection efficiencies were normalized by co-transfection with pEGFP DNA (Clontech).

PKC activity. Total cellular PKC activity was monitored using the PepTag® non-radioactive assay kit (Promega) according to the manufacturer's specifications. Assays for individual PKC isozyme activity were performed as described previously in reference 53.

Statistics. Statistical analysis was performed with analysis of variance (ANOVA) followed by the two-tailed multiple t-test with Bonferroni correction and χ^2 test followed by multiple Fisher's exact test or χ^2 test with Bonferroni correction. The differences were considered to be significant if $p < 0.05$. All error bars are SE, and represent at least 3 independent experiments for IB or 6 independent experiments for cell counting (eight microscopic fields containing at least 80 cells/field).

Acknowledgements

We thank Goberdhan P. Dimri and Robert Benezra for support and technical advice, Philip W. Hinds and Marcelo Kazanietz for discussing unpublished work, Eiji Hara for PKC plasmids, Kaoru Hazeki for PKCδ-shRNA plasmids, Janet Morgan for reagents, David Goodrich for critical reading of the manuscript and Mary Vaughan for expert IHC services. This work was supported by CA94108 and DOD Prostate Cancer Awards W81XWH-08-1-0026 and W81XWH-07-1-0184 (I.H.G.), and in part, by the NCI Cancer Center Support Grant to the Roswell Park Cancer Institute (CA016056).

Note

Supplementary materials can be found at:
www.landesbioscience.com/supplement/AkakuraCC9-23-sup.pdf

References

1. Passos JF, Simillion C, Hallinan J, Wipat A, von Zglinicki T. Cellular senescence: Unravelling complexity. Age (Dordr) 2009; 31:353-63.
2. Caino MC, Meshki J, Kazanietz MG. Hallmarks for senescence in carcinogenesis: Novel signaling players. Apoptosis 2009; 14:392-408.
3. Ben Porath I, Weinberg RA. The signals and pathways activating cellular senescence. Int J Biochem Cell Biol 2005; 37:961-76.
4. Gelman IH. The role of the SSeCKS/Gravin/AKAP12 scaffolding proteins in the spaciotemporal control of signaling pathways in oncogenesis and development. Front Biosci 2002; 7:1782-97.
5. Lin X, Nelson PJ, Frankfort B, Tombler E, Johnson R, Gelman IH. Isolation and characterization of a novel mitogenic regulatory gene, 322, which is transcriptionally suppressed in cells transformed by *src* and *ras*. Mol Cell Biol 1995; 15:2754-62.
6. Lin X, Tombler E, Nelson PJ, Ross M, Gelman IH. A novel *src*- and *ras*-suppressed protein kinase C substrate associated with cytoskeletal architecture. J Biol Chem 1996; 271:28.
7. Chapline C, Mousseau B, Ramsay K, Duddy S, Li Y, Kiley SC, et al. Identification of a major protein kinase C-binding protein and substrate in rat embryo fibroblasts—Decreased expression in transformed cells. J Biol Chem 1996; 271:6417-22.
8. Chapline C, Cottom J, Tobin H, Hulmes J, Crabb J, Jaken S. A major, transformation-sensitive PKC-binding protein is also a PKC substrate involved in cytoskeletal remodeling. J Biol Chem 1998; 273:19482-9.
9. Nauert J, Klauck T, Langeberg LK, Scott JD. Gravin, an autoantigen recognized by serum from myasthenia gravis patients, is a kinase scaffolding protein. Current Biology 1997; 7:52-62.
10. Tchernitsa OI, Zuber J, Sers C, Brinckmann R, Britsch SK, Adams V, et al. Gene expression profiling of fibroblasts resistant toward oncogene-mediated transformation reveals preferential transcription of negative growth regulators. Oncogene 1999; 18:5448-54.
11. Lin X, Gelman IH. Calmodulin and cyclin D anchoring sites on the *Src*-Suppressed C Kinase Substrate, SSeCKS. Biochem Biophys Res Commun 2002; 290:1368-75.
12. Su B, Bu Y, Engelberg D, Gelman IH. SSeCKS/Gravin/AKAP12 inhibits cancer cell invasiveness and chemotaxis by suppressing a PKC-RAF/MEK/ERK pathway. J Biol Chem 2010; 285:4578-86.

13. Piontek J, Brandt R. Differential and regulated binding of PKA and PKC isoenzymes to gravin in human model neurons: Evidence that gravin provides a dynamic platform for the localization of kinases during neuronal development. J Biol Chem 2003; 278:38970-9.
14. Tao J, Wang HY, Malbon CC. Protein kinase A regulates AKAP250 (gravin) scaffold binding to the beta2-adrenergic receptor. EMBO J 2003; 22:6419-29.
15. Akakura S, Huang C, Nelson PJ, Foster B, Gelman IH. Loss of the SSeCKS/Gravin/AKAP12 gene results in prostatic hyperplasia. Cancer Res 2008; 68:5096-103.
16. Lin X, Nelson P, Gelman IH. Regulation of G→S Progression by the SSeCKS tumor suppressor: Control of cyclin D expression and cellular compartmentalization. Mol Cell Biol 2000; 20:7259-72.
17. Chen Z, Trotman LC, Shaffer D, Lin HK, Dotan ZA, Niki M, et al. Crucial role of p53-dependent cellular senescence in suppression of Pten-deficient tumorigenesis. Nature 2005; 436:725-30.
18. Dimri GP, Lee X, Basile G, Acosta M, Scott G, Roskelley C, et al. A biomarker that identifies senescent human cells in culture and in aging skin in vivo. Proc Natl Acad Sci USA 1995; 92:9363-7.
19. Baker DJ, Jeganathan KB, Cameron JD, Thompson M, Juneja S, Kopecka A, et al. BubR1 insufficiency causes early onset of aging-associated phenotypes and infertility in mice. Nat Genet 2004; 36:744-9.
20. Nelson PJ, Moissoglu K, Vargas JJ, Klotman PE, Gelman IH. Involvement of the protein kinase C substrate, SSeCKS, in the actin-based stellate morphology of mesangial cells. J Cell Sci 1999; 112:361-70.
21. Campisi J, d'Adda dF. Cellular senescence: when bad things happen to good cells. Nat Rev Mol Cell Biol 2007; 8:729-40.
22. Hinds PW, Weinberg RA. Tumor Suppressor Genes. Curr Opin Genet Dev 1994; 4:135-41.
23. Krizhanovsky V, Xue W, Zender L, Yon M, Hernando E, Lowe SW. Implications of cellular senescence in tissue damage response, tumor suppression and stem cell biology. Cold Spring Harb Symp Quant Biol 2008; 73:513-22.
24. Funk JO, Waga S, Harry JB, Espling E, Stillman B, Galloway DA. Inhibition of CDK activity and PCNA-dependent DNA replication by p21 is blocked by interaction with the HPV-16 E7 oncoprotein. Genes Dev 1997; 11:2090-100.
25. Grove BD, Bruchey AK. Intracellular distribution of gravin, a PKA and PKC binding protein, in vascular endothelial cells. J Vasc Res 2001; 38:163-75.
26. Ohtani N, Yamakoshi K, Takahashi A, Hara E. The $p16^{INK4a}$-RB pathway: Molecular link between cellular senescence and tumor suppression. J Med Invest 2004; 51:146-53.
27. Ohtani N, Zebedee Z, Huot TJ, Stinson JA, Sugimoto M, Ohashi Y, et al. Opposing effects of Ets and Id proteins on $p16^{INK4a}$ expression during cellular senescence. Nature 2001; 409:1067-70.
28. Ushio K, Hashimoto T, Kitamura N, Tanaka T. Id1 is downregulated by hepatocyte growth factor via ERK-dependent and ERK-independent signaling pathways, leading to increased expression of $p16^{INK4a}$ in hepatoma cells. Mol Cancer Res 2009; 7:1179-88.
29. Bothos J, Tuttle RL, Ottey M, Luca FC, Halazonetis TD. Human LATS1 is a mitotic exit network kinase. Cancer Res 2005; 65:6568-75.
30. Yang X, Yu K, Hao Y, Li DM, Stewart R, Insogna KL, et al. LATS1 tumor suppressor affects cytokinesis by inhibiting LIMK1. Nat Cell Biol 2004; 6:609-17.
31. Takahashi A, Ohtani N, Yamakoshi K, Iida S, Tahara H, Nakayama K, et al. Mitogenic signalling and the $p16^{INK4a}$-Rb pathway cooperate to enforce irreversible cellular senescence. Nat Cell Biol 2006; 8:1291-7.
32. Fridman AL, Tainsky MA. Critical pathways in cellular senescence and immortalization revealed by gene expression profiling. Oncogene 2008; 27:5975-87.
33. Bhatia B, Jiang M, Suraneni M, Patrawala L, Badeaux M, Schneider-Broussard R, et al. Critical and distinct roles of p16 and telomerase in regulating the proliferative life span of normal human prostate epithelial progenitor cells. J Biol Chem 2008; 283:27957-72.
34. Larochelle DA, Vithalani KK, De Lozanne A. A novel member of the *rho* family of small GTP-binding proteins is specifically required for cytokinesis. J Cell Biol 1996; 133:1321-9.
35. Saito S, Tatsumoto T, Lorenzi MV, Chedid M, Kapoor V, Sakata H, et al. Rho exchange factor ECT2 is induced by growth factors and regulates cytokinesis through the N-terminal cell cycle regulator-related domains. J Cell Biochem 2003; 90:819-36.
36. Saurin AT, Durgan J, Cameron AJ, Faisal A, Marber MS, Parker PJ. The regulated assembly of a PKCepsilon complex controls the completion of cytokinesis. Nat Cell Biol 2008; 10:891-901.
37. Gelman IH, Lee K, Tombler E, Gordon R, Lin X. Control of cytoskeletal architecture by the *src*-suppressed C kinase substrate, SSeCKS. Cell Motil Cytoskeleton 1998; 41:1-17.
38. Gelman IH, Gao L. The SSeCKS/Gravin/AKAP12 metastasis suppressor inhibits podosome formation via rhoA- and Cdc42-dependent pathways. Molecular Cancer Research 2006; 4:151-8.
39. Xia W, Gelman IH. Mitogen- and FAK-regulated tyrosine phosphorylation of the SSeCKS scaffolding protein modulates its actin-binding properties. Exp Cell Res 2002; 277:139-51.
40. Choi MC, Lee YU, Kim SH, Park JH, Kim HA, Oh DY, et al. A-kinase anchoring protein 12 regulates the completion of cytokinesis. Biochem Biophys Res Commun 2008; 373:85-9.
41. Takahashi A, Ohtani N, Hara E. Irreversibility of cellular senescence: Dual roles of $p16^{INK4a}$/Rb-pathway in cell cycle control. Cell Div 2007; 2:10.
42. Swift S, Lorens J, Achacoso P, Nolan GP. Rapid production of retroviruses for efficient gene delivery to mammalian cells using 293T cell-based systems. Curr Protoc Immunol 2001; 10:17; PubMed PMID: 18432682.
43. Morgenstern JP, Land H. Advanced mammalian gene transfer: High titre retroviral vectors with multiple drug selection markers and a complementary helper- free packaging cell line. Nucl Acids Res 1990; 18:3587-96.
44. Su B, Zheng Q, Vaughan MM, Bu Y, Gelman IH. SSeCKS metastasis-suppressing activity in MatLyLu prostate cancer cells correlates with VEGF inhibition. Cancer Res 2006; 66:5599-607.
45. Moissoglu K, Sachdev S, Gelman IH. Enhanced v-Src-induced oncogenic transformation in the absence of focal adhesion kinase is mediated by phosphatidylinositol 3-kinase. Biochem Biophys Res Commun 2005; 330:673-84.
46. Bihani T, Chicas A, Lo CP, Lin AW. Dissecting the senescence-like program in tumor cells activated by Ras signaling. J Biol Chem 2007; 282:2666-75.
47. Hahn WC, Dessain SK, Brooks MW, King JE, Elenbaas B, Sabatini DM, et al. Enumeration of the simian virus 40 early region elements necessary for human cell transformation. Mol Cell Biol 2002; 22:2111-23.
48. Iwabu A, Smith K, Allen FD, Lauffenburger DA, Wells A. Epidermal growth factor induces fibroblast contractility and motility via a protein kinase C delta-dependent pathway. J Biol Chem 2004; 279:14551-60.
49. Hazeki K, Inoue K, Nigorikawa K, Hazeki O. Negative regulation of class IA phosphoinositide 3-kinase by protein kinase Cdelta Limits Fcgamma receptor-mediated phagocytosis in macrophages. J Biochem 2009; 145:87-94.
50. Gelman IH, Tombler E, Vargas J Jr. A role for SSeCKS, a major protein kinase C substrate with tumor suppressor activity, in cytoskeletal architecture, formation of migratory processes and cell migration during embryogenesis. Histochem J 2000; 32:13-26.
51. Matsui S, Yoshida H, Weinfeld H, Sandberg AA. Induction of prophase in interphase nuclei by fusion with metaphase cells. J Cell Biol 1972; 54:120-32.
52. Karpf AR, Matsui S. Genetic disruption of cytosine DNA methyltransferase enzymes induces chromosomal instability in human cancer cells. Cancer Res 2005; 65:8635-9.
53. Rodriguez EM, Dunham EE, Martin GS. Atypical protein kinase C activity is required for extracellular matrix degradation and invasion by Src-transformed cells. J Cell Physiol 2009; 221:171-82.